

Critical Strain Determination Based on the Euler-Fresnel Jig

Sotiris Koussios¹, Katrin Tazelaar², N.Bert Roozen³, René C. Alderliesten¹, Adriaan Beukers¹

¹Department of Structural Integrity and Composites, Faculty of Aerospace Engineering,
Delft University of Technology, Delft, The Netherlands

²Composites Laboratory, InHolland University of Applied Sciences, Delft, The Netherlands

³Katholieke Universiteit Leuven, Laboratory of Acoustics, Soft Matter and Biophysics, Department of
Physics and Astronomy, Celestijnenlaan 200 D, B-3001 Leuven, Belgium

Track 6-1: New Structural Testing Methods

ABSTRACT

When considering a composite strip or plate under certain thermal and environmental conditions and loadings, there is a minimum strain threshold for the appearance of the first micro crack. The associated strain level is defined here as “critical strain”.

There are various active displacement methods to measure this strain level (by tension and bending). The registration of the first micro crack is however challenging. Therefore, some alternative methods have been developed like the Bergen ellipse [1]. With this method, a relatively thin strip is forced by clamping to “follow” the elliptical contour of the jig. The strip undergoes various strain levels from 0% to 2% or 3%. However, the strain distribution as a function of the strip length is far from linear. This causes inaccurate readings and high error sensitivity for certain areas on the ellipse.

To overcome this problem, a novel jig design is introduced here; this design is based on a perfectly linear strain distribution along the strip's length. The resulting curve is a classical one known as the Euler-Fresnel curve [2]. The linearity and the constant, low sensitivity to measurement errors guarantees high accuracy. Only at the beginning and the end of the strip, the measured strain might deviate from the real one, especially when the thickness of the strip is moderately less ($\Delta h > 0.1$ [mm]) than the height of the slot, Figure 9. The jig is a low cost device that can easily be placed in climate cabinets for e.g. cryo-cycling.

In this paper we focus on the mathematical derivation of the jig, compare it to the Bergen ellipse, and provide the full consideration of the associated primary and secondary forces and moments. In addition, a comprehensive strength analysis of various lay-ups is provided for the maximum strain level of 2%. The paper ends with some key conclusions and recommendations.

1 INTRODUCTION

The introduction of composites in the aerospace industry has led to significant spin-off in automotive applications, manufacturing of sporting goods, the introduction of civil applications, pressure vessels and piping, and general machine building. In particular the last decade, the amount of composites in aircraft structures has passed the 50% limit (by weight) and has therefore triggered some interesting discussions regarding the numbers behind design allowables, experimental methods for their determination, and advanced failure propagation analysis methods like XFEM and the use of cohesive elements.

The classical damage classification, as presented in textbooks about composite mechanics is based on two definitions: FPF (first ply failure) and LPF (last ply failure, which is usually detected by a progressive damage analysis procedure). Next to these classifications, a significant number of other damage phenomena can take place. Although the definition of “damage” is application-dependent but is also formed by experience and, up to some extent, tradition, there are numerous material integrity changes that can be regarded as damage phenomena. These are crazing, void forming, microcracking and invisible delaminations (typically as a result of impact).

Micro cracking takes place in a quite early stage of the loading process. While the typical tension strength of a UD Carbon-Epoxy laminate is above 1500 [MPa] (which corresponds to app. 1% strain),

microcracks (which are audible during a tension experiment) take place at strain levels of even 0.4%. The determination of these cracking phenomena is difficult to “catch” as the tension experiment immediately proceeds to further displacement. To accurately determine the level of the first microcrack, a method is needed in which the laminate is statically loaded by a complete spectrum of strain levels, starting at 0% and ending at e.g. 2%. For this, specially defined curves [1] can be constructed that serve as a support on which the composite strip is clamped. The occurrence of the first microcrack, craze or void is accompanied with a minimum strain value which will be called here “critical strain”. There is a plethora of (application-dependent) definitions for this; the definition presented here is based on the detection of micro-cracks in painted composite substrates. The challenge was to investigate where the cracks initiate and how they propagate through the paint or through the substrate.

For the determination of the critical strain, a suitable method that puts the specimen under a broad strain spectrum is the so-called Bergen ellipse [2], Fig. 3. The strip is clamped over the top of the ellipse and undergoes various degrees of curvature which are directly coupled to (bending) strain. Despite the fact that the Bergen ellipse may be considered a classic in the composites world, there are several disadvantages. The curvature, as a function of the curve length, is far from linear [3]. This has profound implications on the measurement sensitivity and accuracy. In addition, the sharp curvature at the vicinity of the horizontal major axis raises problems for the clamping of the strip which, in most cases, will not be able to follow the contour.

To resolve these issues we propose here a “novel” curve shape, known as the Euler-Fresnel curve [4], Fig. 4. This curve has the unique property of a curvature distribution that is a perfectly linear function of the contour length. Therefore, the measurement accuracy, linearity and sensitivity do not form an issue anymore. In addition, the specimen is not clamped but inserted in a specially machined slot to guarantee perfect matching with the underlying shape. The only issue is, that the last 10 [mm] of the curve do not provide accurate readings anymore because the strip will not perfectly follow mathematics, which state that the curvature at the very end of the strip is maximal (the same applies on the Bergen ellipse).

After a short introduction in 2D curve geometry, the novel Euler-Fresnel jig is compared to the Bergen ellipse in terms of curvature distribution and global dimensions. Next, a procedure is provided regarding strain measurements and the design of such a jig. The design is based on two parameters: the thickness h of the specimen and the desired maximum strain ϵ . Depending on the lay-up of the specimen, secondary loadings might occur when loading the strip in bending (by placing it in the jig). These loads are quantified while the strength of the specimen is assessed in terms of the maximum strain and the Tsai-Hill criteria. The conclusion is that the method works very well but care is needed for the selection of appropriate laminates for negligible secondary loading which would lead to multi-axial stress fields and therefore inaccurate readings.

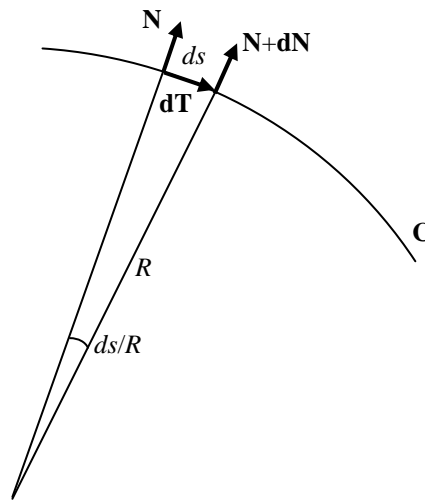


Figure 1: A 2-D curve C and its characteristic vectors and radius of curvature

2 TWO-DIMENSIONAL CURVE GEOMETRY

The general definition of a 2D parametric curve is [1]:

$$\mathbf{C}(t) = \{x(t), y(t)\}, \quad t_0 \leq t \leq t_1 \quad (1)$$

The independent parameter t is not necessarily expressing a specific property of the curve (like the length along its path or an orientation angle). An important property of a curve is its length s which we express here as a function of the independent parameter t :

$$s(t) = \int_{t_0}^t \underbrace{\sqrt{(x'(\eta))^2 + (y'(\eta))^2}}_{ds} d\eta \quad (2)$$

where η is the integration variable and t_0 the begin value of the integration interval.

Another important property of a curve is its curvature; this parameter expresses the rate of direction change as a function of the independent curve parameter t :

$$k(t) = \frac{1}{R(t)} = \frac{x'(t)y''(t) - y''(t)x'(t)}{\left((x'(t))^2 + (y'(t))^2\right)^{3/2}} \quad (3)$$

A more convenient way to handle curvature is to express it as a function of the curve's length. This way, the ability is created to calculate the direction change of the curve over a step ds . This expression has thus a physical meaning. It is however not always possible to derive the required expressions without increasing the complexity of the involved equations.

To completely assess a curve in the two dimensional plane, the tangent vector \mathbf{T} and the normal vector \mathbf{N} are important ingredients:

$$\mathbf{T}_{\text{clockwise}} = \frac{1}{ds} \begin{Bmatrix} x'(t) \\ -y'(t) \end{Bmatrix}, \quad \mathbf{N}_{\text{outward}} = \frac{1}{ds} \begin{Bmatrix} y'(t) \\ x'(t) \end{Bmatrix} \quad (4)$$



Figure 2: Example of a continuous strain Euler-Fresnel jig. The specimen (not shown here) is clamped under the two straps. Courtesy: TESLA motors.

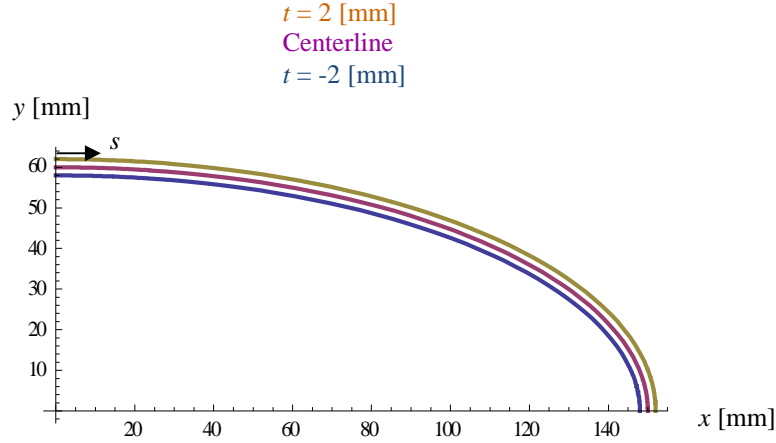


Figure 3: The Bergen ellipse (central curve) and the upper and lower offset curves caused by the thickness of the specimen (4 [mm]).

where the plus and minus signs depend on the s -direction and on the side in which \mathbf{N} is pointing. An important property is: $\mathbf{T} \cdot \mathbf{N} = 0$. The curvature definition can be coupled to these vectors according to Fig. 1. The radius of curvature R is the length over which two adjacent normal vectors \mathbf{N} and $\mathbf{N} + d\mathbf{N}$ intersect each other. The distance between these normal vectors is ds in the direction $d\mathbf{T}$. The enclosed angle is approximately equal to ds/R .

3 JIGS FOR STRAIN MEASUREMENTS

To expose a composite or polymer specimen to a variety of strain levels in a simultaneous way, a thin strip of the considered material is clamped over the curved surface of a specially made jig, Fig. 2. Ideally, the strip should only experience a bending curvature over the length of the top curve but, as we will derive later, there is usually a number of secondary loadings active that depend on the material properties and the lay-up of the specimen.

3.1 The Bergen Ellipse

One of the first known experiments for continuous strain measurement is resembled by the so-called Bergen ellipse [2]. Its geometry is given by:

$$\mathbf{C}_{\text{Bergen}} = \begin{Bmatrix} A \cos t \\ B \sin t \end{Bmatrix}, \quad 0 \leq t \leq \frac{\pi}{2} \quad (5)$$

with $A = 150$ [mm] and $B = 60$ [mm]. The equation represents the neutral line of the bended strip which is indicated by a purple line (midline) in Fig. 3. When following the curve in the direction from $\{0, 60\}$ to $\{150, 0\}$ (see arrow in Fig. 3), the tangent and normal vectors respectively become [3]:

$$\begin{aligned} \mathbf{T}_{\text{Bergen}}(t) &= \frac{1}{\sqrt{A^2 \cos^2 t + B^2 \sin^2 t}} \begin{Bmatrix} A \sin t \\ -B \cos t \end{Bmatrix} \\ \mathbf{N}_{\text{Bergen}}(t) &= \frac{1}{\sqrt{A^2 \cos^2 t + B^2 \sin^2 t}} \begin{Bmatrix} B \cos t \\ A \sin t \end{Bmatrix} \end{aligned} \quad (6)$$

The curvature of the ellipse is given by:

$$k_{\text{Bergen}}(t) = \frac{AB}{(B^2 \cos^2 t + A^2 \sin^2 t)^{3/2}} \quad (7)$$

As shown later, the curvature distribution over the contour length is strongly non-linear. This implies difficulties for the determination of the strain level at a particular area of the curve. The answer to this problem is the so-called Euler-Fresnel curve, introduced in [4].

3.2 The Euler-Fresnel Curve

Ideally, for a strain measurement with a constant sensitivity to errors, the strain (or in other words the curvature) of the supporting jig should be a linear function of its length:

$$k(t) = \frac{1}{R(t)} = \frac{x'(t)y''(t) - y''(t)x'(t)}{\left((x'(t))^2 + (y'(t))^2\right)^{3/2}} = 2a \int_{t_0}^t \underbrace{\left(\sqrt{(x'(\eta))^2 + (y'(\eta))^2}\right)}_{ds} d\eta \quad (8)$$

where $2a$ is the linearity constant (with the dimension $[\text{mm}^{-2}]$). The solution to the above equation is known as the Euler-Fresnel curve with the following parameterisation:

$$\mathbf{C}(s) = \sqrt{\frac{2\pi}{a}} \left\{ \text{FS}\left(\frac{2a}{\pi}s\right), \text{FC}\left(\frac{2a}{\pi}s\right) \right\}, \quad 0 \leq s \leq \sqrt{\frac{\pi}{a}} \quad (9)$$

$$\text{FS} = \int \sin(as^2) ds \quad \text{FC} = \int \cos(as^2) ds$$

For $s = (\pi/a)^{1/2}$, the curve will cover a total angle of 180° , Fig. 4:

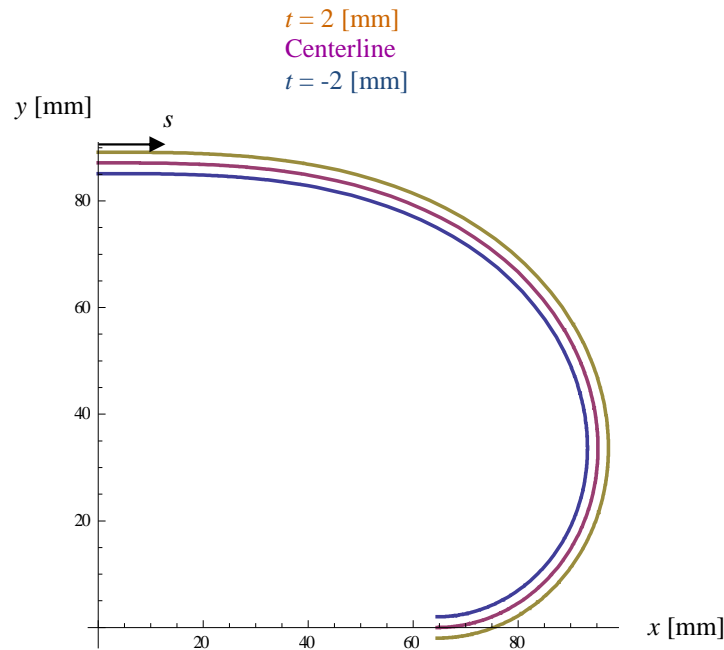


Figure 4: The Euler-Fresnel curve (midline) with a 4 [mm] strip placed on it.

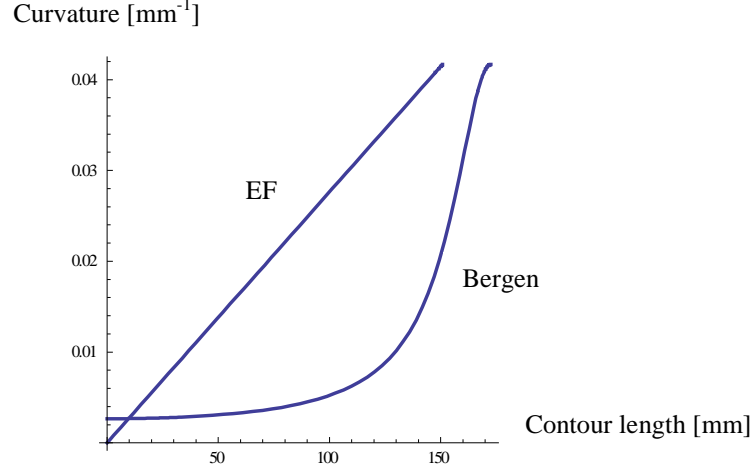


Figure 5: Comparison between the Euler-Fresnel curvature (linear) and the curvature of the Bergen ellipse (exponential) as a function of the contour length for equal k_{\max} values (0.042 [mm⁻¹]).

The tangent and normal vectors (when following the direction of the arrow) are given by:

$$\mathbf{T}_{\text{EF}} = \begin{Bmatrix} \cos(as^2) \\ -\sin(as^2) \end{Bmatrix}, \quad \mathbf{T}_{\text{EF}} = \begin{Bmatrix} \sin(as^2) \\ \cos(as^2) \end{Bmatrix} \quad (10)$$

The curvature must be a linear function of s :

$$k_{\text{EF}}(s) = \frac{x'(s)y''(s) - y''(s)x'(s)}{\left((x'(s))^2 + (y'(s))^2\right)^{3/2}} = 2as \quad (11)$$

The curvatures of the Bergen ellipse and the Euler-Fresnel curve are compared in Fig. 5 for a maximum curvature value of 0.042 [mm⁻¹]. The advantage of the Euler-Fresnel curve becomes clear as it resembles perfect linearity for $k(s)$. The global dimensions of both contours are comparable; for the same maximum curvature they fit in to a parallelogram of [80×150] [mm]. The length of the EF curve is here 150.8 [mm] (Bergen = 172.6 [mm]). The contour lengths are respectively calculated with:

$$s_{\max, \text{EF}} = 2as \Big|_{s=\sqrt{\frac{\pi}{a}}} = 2\sqrt{\pi a}, \quad s_{\max, \text{Bergen}} = B E_{\text{Elliptic}} \left(\theta, 1 - \frac{A^2}{B^2} \right) \Big|_{\theta=\frac{\pi}{2}} = B E_{\text{Elliptic}} \left(1 - \frac{A^2}{B^2} \right) \quad (12)$$

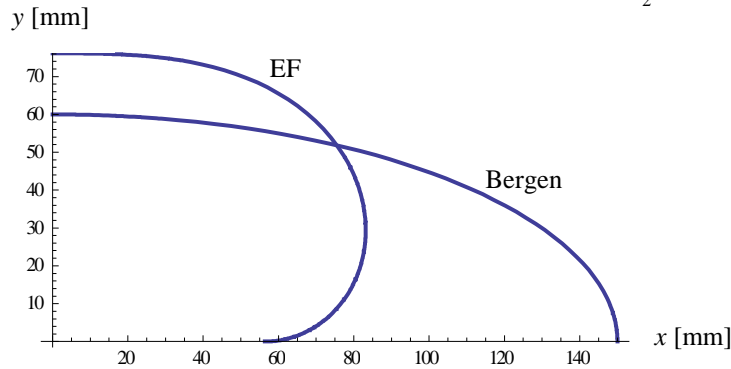


Figure 6: Comparison of the EF curve to the Bergen ellipse for a common maximum k of 0.042 [mm⁻¹]

where $E_{\text{elliptic}} = E(\phi|m) = \int (1 - m \sin^2 \theta)^{1/2} d\theta$, integrated over the interval $[0, \phi]$ for $-\pi/2 < \phi < \pi/2$ with $E(m) = E(\pi/2, m)$. This integral is an elliptic one of the second kind [5]. For equal length ($= 172.6$ [mm]), the Bergen curve is able to reach a curvature of 0.0417 [mm^{-1}] while the EF curvature will attain the value of 0.036 [mm^{-1}].

3.3 Strain Measurements on the EF Curve

The curvature over the Euler-Fresnel (EF) curve starts at 0 (top-left end) and increases until a prescribed maximum value $k_{\text{max,EF}}$ which depends on the parameter a , Eq. (12). Assuming the neutral line in the middle of the cross section of the strip, Fig. 4, the strain can simply be determined by:

$$\epsilon_{\text{EF}}(s, z) = 2asz, \quad \begin{aligned} 0 \leq s \leq \sqrt{\frac{\pi}{a}} \\ -\frac{h}{2} \leq z \leq \frac{h}{2} \end{aligned} \quad (13)$$

This equation is only valid for either isotropic or reasonably symmetric anisotropic materials where the neutral line is indeed approximately located in the middle of the thickness. The result of it is depicted in Fig. 7. Regardless the position of this line, all candidate materials are here assumed to be perfectly linearly elastic while the bending is based on the assumption that the normals remain straight and vertical to the elastic line. For isotropic materials, the bending stress is given by:

$$\sigma(s, z) = \frac{M(s, z)z}{I} \quad \text{with} \quad M(s, z) = k_{\text{EF}}(s, z)EI \quad (14)$$

Alternatively, one can immediately use: $\sigma = 2Easz$ (Eq. (13)).

3.4 Euler Fresnel Curve Design

The design of the EF curve can be entirely captured by two parameters:

- The shape factor a [mm^{-2}]
- The maximum length s_{max} .

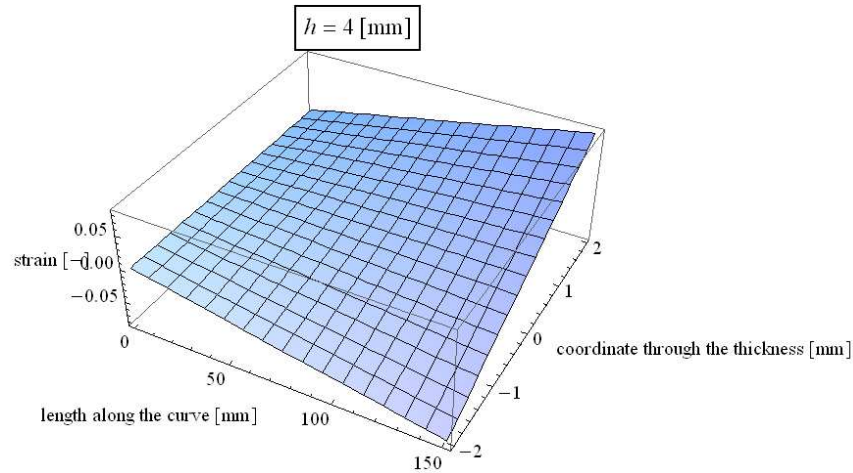


Figure 7: The strain [-] of a strip that is mounted on the EF jig as a function of the jig length s and the thickness h .

For convenience, the curve is designed in such a way that it covers a total angle of 180° . The reasons behind this choice reflect on machining and handling of the jig. Therefore, the maximum length is fixed to $(\pi/a)^{1/2}$.

For a strip with a total thickness h and desired maximum strain e , the parameter a_{req} becomes:

$$e = 2a_{\text{req}} \sqrt{\frac{\pi}{a_{\text{req}}}} \frac{h}{2} \rightarrow a_{\text{req}} = \frac{e^2}{h^2 \pi} \quad (15)$$

with a_{req} , the maximum curve length becomes:

$$s_{\text{max}} = \pi \frac{h}{e} \quad (16)$$

while the maximum curvature is:

$$k_{\text{max}} = \frac{2e}{h} \quad (17)$$

Compared to the jig geometry as presented in [4], the relations are here much simpler because the neutral line is now placed in the middle of the strip's cross section. In addition, the measurement error, as reported in the same work, has now disappeared while the machining has also been simplified since a tool with a diameter equal to the specimen's thickness should follow the EF curve and not its offset (by $h/2$). For $e = 2\%$ and $h = 2$ [mm] (same values as in [4]) the jig attains the form as given in Figure 8. The shape parameter is here equal to $1/(\pi \times 10^5)$ [mm⁻²]; the maximum length is $100 \times \pi$ [mm].

4 APPLICATION TO COMPOSITES

4.1 Load Analysis

As previously mentioned, the simple, elegant equations (13) and (14) apply only on isotropic materials or composites for which the conditions of symmetry and balance apply. Even for this category, situations might arise in which the secondary loadings (induced by bending) are not negligible anymore.

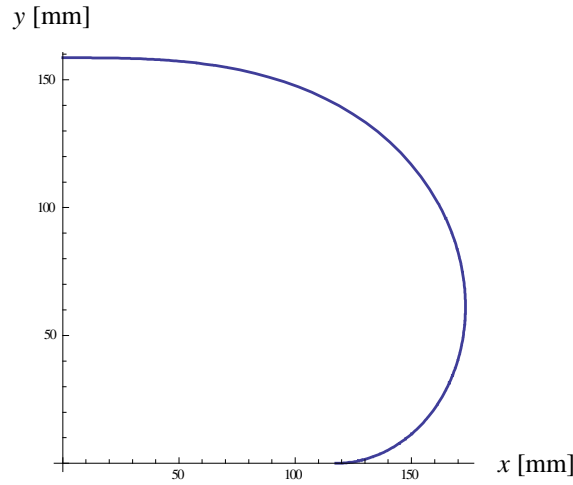


Figure 8: The Euler-Fresnel jig for $e = 2\%$ and $h = 2$ [mm]



Figure 9: Euler-Fresnel jig as manufactured, including a spindle for pushing the strip into the curved slot (example for $h = 2.5$ [mm])

Since the definition of “critical strain” is based on a pure mono-dimensional bending deformation, the candidate laminates should be examined on secondary loadings and the thereby induced stresses and strains. The first step is to accurately define the properties of the real manufactured jig as presented in Figure 9. The jig consists of the following parts: the curve with a specially machined slot to accommodate the strip, and a spindle to push the strip into this slot. The slot geometry is now assumed as: $b = 20$ [mm] and $h = 2$ [mm] with $l = 100 \times \pi$ [mm]. Based on these dimensions, a possible specimen geometry could be: $l = 99 \times \pi \pm 3$, [mm], $b = 19.9 \pm 0.1$ [mm], $t = 1.98 \pm 0.02$ [mm]. According to the classical lamination theory, the deformation of the relatively thick composite strip (with a considerable width, say 20 [mm]) is given by [6]:

$$\begin{Bmatrix} N_x \\ N_y \\ N_{xy} \\ M_x \\ M_y \\ M_{xy} \end{Bmatrix} = \begin{bmatrix} \mathbf{A} & \mathbf{B} \\ \mathbf{B} & \mathbf{D} \end{bmatrix} \cdot \begin{Bmatrix} \varepsilon_x \\ \varepsilon_y \\ \gamma_{xy} \\ \kappa_x \\ \kappa_y \\ 2\kappa_{xy} \end{Bmatrix}, \quad \text{with} \quad \begin{cases} \mathbf{A} = \sum_{k=1}^n \mathbf{C}_k (z_k - z_{k-1}) \\ \mathbf{B} = \frac{1}{2} \sum_{k=1}^n \mathbf{C}_k (z_k^2 - z_{k-1}^2) \\ \mathbf{D} = \frac{1}{3} \sum_{k=1}^n \mathbf{C}_k (z_k^3 - z_{k-1}^3) \end{cases} \quad (18)$$

where:

$$z_k = \sum_{i=1}^k t_i - \frac{h}{2}, \quad z_0 = -\frac{h}{2}, \quad h = \sum_{k=1}^n t_k, \quad \mathbf{C}_k = \mathbf{M}_k \cdot \mathbf{Q} \cdot \mathbf{M}_k^T, \quad \mathbf{Q} = \begin{bmatrix} \frac{E_x}{1 - \mu_{xy}\mu_{yx}} & \frac{\mu_{xy}E_y}{1 - \mu_{xy}\mu_{yx}} & 0 \\ \frac{\mu_{xy}E_y}{1 - \mu_{xy}\mu_{yx}} & \frac{E_y}{1 - \mu_{xy}\mu_{yx}} & 0 \\ 0 & 0 & G_{xy} \end{bmatrix}, \quad (19)$$

$$\mathbf{M}_k = \begin{bmatrix} \cos^2 \varphi_k & \sin^2 \varphi_k & 2 \cos \varphi_k \sin \varphi_k \\ \sin^2 \varphi_k & \cos^2 \varphi_k & -2 \cos \varphi_k \sin \varphi_k \\ -\cos \varphi_k \sin \varphi_k & \cos \varphi_k \sin \varphi_k & \cos^2 \varphi_k - \sin^2 \varphi_k \end{bmatrix}$$

The positive directions for $N_{\#}$ [N/mm] and $M_{\#}$ [N×mm/mm] and their corresponding strains / curvatures are given below:

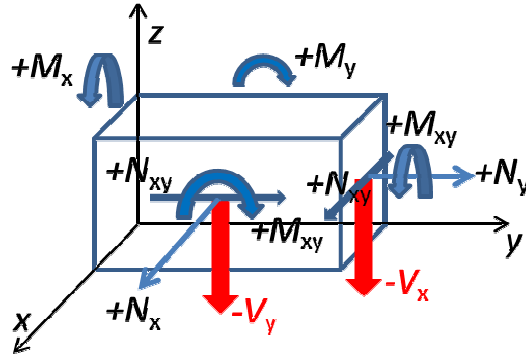


Figure 10: Positive directions for applied loads and moments on an elementary laminate piece

It is now assumed that the jig curve direction coincides with the x -axis. The laminate which is examined for secondary loadings has the following mechanical properties:

Table 1: Mechanical properties of the examined Carbon/Epoxy laminate

E_x	[GPa]	145
E_y	[GPa]	7
μ_{xy}	[-]	0.34
G_{xy}	[GPa]	3.5
X_{tensile}	[MPa]	1750
$X_{\text{compressive}}$	[MPa]	-1350
Y_{tensile}	[MPa]	63
$Y_{\text{compressive}}$	[MPa]	-210
T_{shear}	[MPa]	80

Depending on its lay-up, the strip will not only experience the dominant bending load M_x , but also secondary loadings which, in some cases, are not negligible. The full ABD analysis is summarized in the table below:

Table 2: Main and secondary loads on a strip placed in the Euler-Fresnel jig.

$$h = 2 \text{ [mm]}, \varepsilon(s_{\max}, h/2) = 2\%, \mathbf{M} = 1000 \text{ [N}\times\text{mm/mm]}$$

Lay-up	0° / 90° symm	0°/90° anti symm	± 45° symm	± 45° anti symm	Q.I symm	Q.I anti symm	UD 0°	UD 10°	UD 45°	UD 80°	UD 90°
N_x	0	-M/3	0	0	0	0	0	0		0	0
N_y	0	0	0	0	0	0	0	0		0	0
N_{xy}	0	0	0	-M/6	0	-M/11	0	0		0	0
M_x	1.3M	M	M/2	M/2	1.2M	1.2M	2M	1.8M	M/2	M/10	M/10
M_y	M/31	M/31	M/2	M/2	M/11	-M/11	M/31	M/12	M/2	M/12	M/30
M_{xy}	0	0	M/6	0	M/23	0	0	-M/3	-M/2	-M/67	0

The bold numbers indicate the desired bending loading, while the colours red, orange, blue and green stand for respectively the following secondary loading gradations: severe, moderate, low, entirely negligible. For the calculations we assumed here that every strain or curvature mode, except k_x , is 100% restricted. This is a very conservative approach. In reality, the deformation constraints are the ones given in Table 3.

Table 3: Kinematic restrictions on the strip, placed in the jig slot

Mode	Restriction
ε_x	No
ε_y	Unlikely, unless Poisson effect of the compressed side leads to $b_{\text{strip}} > b_{\text{slot}}$
γ_{xy}	Partially, if the laminate is non-balanced and the shear leads to a rhombus not fitting in b
k_x	This is entirely dictated by the EF jig
k_y	No, because of slot geometry
k_{xy}	Partially, especially by symmetric laminates that contain soft (angleply) layers

4.2 Strength Analysis

The examined strain level is 2%. This is beyond the limits of the average carbon/UD layer. The Euler-Fresnel jig is primarily designed to detect the minimum stress or strain level at which the first microcrack will appear on the top layer of the examined laminate. At the exact location of the first microcrack, the layers below should not yet reach a level in which extensive damage can take place.

For the 2% strain level, an analysis, based on the maximum strain and Tsai-Hill criteria has revealed some interesting results: soft laminates are better capable of handling high strain levels than “hard” ones like cross-ply. We have examined here laminates consisting of 8 layers with an individual thickness of 0.25 [mm]. The results are summarised in the table below where H and e stand for failure according to the Tsai-Hill or the maximum strain criterion respectively. The allowable strain levels are estimated by dividing the appropriate stress allowables (tensile or compressive) by the corresponding stiffness elements. These values are certainly higher than experimental limits for the strain. Nevertheless, the maximum strain criterion is still conservative as compared to the Tsai-Hill results.

Table 4: Failed layers for a 2% strain level. 1 = top layer (tension), 8 = bottom layer (compression)

Lay-up Failed layer #	0° / 90° symm	0°/90° anti symm	± 45° symm	± 45° anti symm	Q.I Symm	Q.I Anti symm	UD 0°	UD 10°	UD 45°	UD 80°	UD 90°
1	H, e	H, e			H, e	H, e	H, e	H, e			
2							e	e			
3											
4											
5											
6											
7	e	e			e	e	e	e		e	e
8	e	H, e			e	e	e	e		H, e	H, e

In regard to the UD layers it is remarkable that failure only occurs when the angle is outside the interval [30°, 60°]. The soft ±45° angleply survives as well but every “hard” laminate fails due to its relative high stiffness in the bending direction. Depending on the occurring stress (tensile or compressive) the appropriate stress allowable is here selected. This is the reason for the lack of symmetry when comparing the top layer related results to the bottom layer related ones.

5 CONCLUSIONS

In this paper we have outlined a novel method to measure critical strain. The method is based on a jig where a composite strip is inserted. The strip undergoes bending whereby the curvature is a linear function of the strip's length. At some point, the first crack will appear. The strain level corresponding to the crack location is called the "critical strain".

After the derivation of the jig shape and its comparison to existing alternatives, a design method is provided to create jigs for specific laminate thickness values and specific desired maximum strain levels. Next, a variety of typical laminates has been assessed on the occurrence of primary (due to bending) and secondary (due to kinematic restrictions) loadings in which it is demonstrated that some layups do not provide reliable results for the critical strain due to the generation of a multi-axial stress field. Furthermore, a strength analysis, based on the maximum strain and Tsai-Hill criteria has shown that "soft" laminates (dominated by angleply layers with angles in the interval $[30^\circ, 60^\circ]$) are less prone to cracking than hard laminates (dominated by cross ply layers). The method has also been evaluated in terms of applicability and accuracy, however, the results of these procedures are not presented here.

In conclusion, the proposed jig method for the determination of the critical strain is characterised by high accuracy, convenient handling, perfect linearity, high accuracy and suitability for exposure to various environmental conditions. The only drawback is the need to machine the jig for which, however, the design depends only on two parameters. For $h = \{1.5, 2, 2.5\}$ [mm] and $\varepsilon_{\max} = 2\%$, the reader can obtain free .stp files from the Delft University of Technology. The costs for the manufacturing a jig including the spindle are app. 1500 euro.

Despite the encouraging results so far, a more in-depth analysis is needed for the analysis of stresses in the laminate and the strain accuracy in cases where the thickness of the specimen is considerably less than the height of the slot (Figure 9) ($h_{\text{slot}} - h_{\text{specimen}} > 0.1$ [mm]). In addition, a more reliable analysis of secondary loads is highly needed.

ACKNOWLEDGEMENTS

This work has been performed within the 'Cryogenic Hypersonic Advanced Tank Technologies' project investigating tank technologies for high-speed transport. CHATT, coordinated by DLR-SART, is supported by the EU within the 7th Framework Program Theme 7 Transport, Contract no.: ACP1-GA-2011-285117. Further information on CHATT can be found on <http://www.chatt.aero>.

REFERENCES

- [1] Gray A. *Modern Differential Geometry of Curves and Surfaces*. CRC press, 1993.
- [2] Bergen jr, RL. *Stress Cracking*, SPE journal, **24**, pp. 77. (1968).
- [3] Farin G. *Curves and Surfaces for CAD: a Practical Guide*. San Francisco: Morgan Kaufmann Publishers, 2002.
- [4] Tazelaar K, Roozen NB, Koussios S, Beukers A. *A New Method to Measure Critical Strain in Composite Materials-Combining the Euler-Fresnel Spiral with Acoustic Emission to Assess Crack Positions*. Composites Science and Technology, Volume 100, 21 August 2014, Pages 228–236.
- [5] Kreyszig E. *Advanced Engineering Mathematics*. New York: John Wiley & Sons, Inc. 1999.
- [6] Daniel IM, Ori Ishai. *Engineering Mechanics of Composite Materials*. Second Edition. Oxford University Press, New York, Oxford, 2006.